Accepted Manuscript

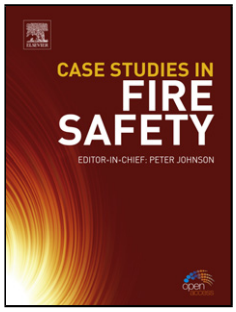

Title: The corrosion behavior of a sputtered micrograin film on Fe-5Cr-5Si alloy in H_2-CO_2-H_2S mixture at 700 °C

Author: L.L. Liu W.B. Li Q.Q. Guo C.S. Ni Y. Niu

PII: S0010-938X(16)30232-3
DOI: http://dx.doi.org/doi:10.1016/j.corsci.2016.05.017
Reference: CS 6778

To appear in:

Received date: 8-1-2016
Revised date: 8-5-2016
Accepted date: 14-5-2016

Please cite this article as: L.L.Liu, W.B.Li, Q.Q.Guo, C.S.Ni, Y.Niu, The corrosion behavior of a sputtered micrograin film on Fe-5Cr-5Si alloy in H2-CO2-H2S mixture at 700°C, Corrosion Science http://dx.doi.org/10.1016/j.corsci.2016.05.017

The corrosion behavior of a sputtered micrograin film on Fe-5Cr-5Si alloy in H_2-CO_2-H_2S mixture at 700 °C

L.L. Liu[a, b], W.B. Li[c], Q.Q. Guo[b], C. S. Ni[d], Y. Niu[b*]

[a] Live Working Center of State Grid Corporation of Hunan, Lixiangzhong Road 8, 410000, Changsha (China)

[b] Institute of Metal Research, Chinese Academy of Sciences, Wencui Road 62, 110016 Shenyang (China)

[c] Hunan Electric Power Corporation Research Institute, Shuidian Road 79, 410000, Changsha (China)

[d] School of Chemistry, University of St Andrews, Fife KY16 9ST, Scotland

[*] Corresponding author. E-mail address: yniu@imr.ac.cn

Highlights

- The as-cast Fe-5Cr-5Si alloy suffers a serious degradation in H_2-CO_2-H_2S at 700°C.
- The sputtered Fe-5Cr-5Si film decreases the corrosion rate of the Fe-5Cr-5Si alloy.
- A thin layer of SiO_2+Cr_2O_3 forms at the coating/alloy interface.
- The formation mechanism of the protective SiO_2+Cr_2O_3 layer is discussed thoroughly

Abstract: The corrosion behaviors of as-cast Fe-5Cr-5Si alloy with and without sputtered Fe-5Cr-5Si film in H_2-CO_2-H_2S mixture at 700°C are studied. The corrosion scale forming on the as-cast alloy is non-protective and mainly composed of FeS outer layer and FeS+$FeCr_2O_4$+Fe_2SiO_4 inner layer. However, a continuous

Cr_2O_3+SiO_2 layer which possesses favorable protectiveness forms at the coating/alloy interface for the coated alloy, even though FeS layer and FeS+$FeCr_2O_4$+Fe_2SiO_4 mixed layer also form. The formation mechanism of the Cr_2O_3+SiO_2 layer on the coated alloy is discussed thoroughly.

Keywords: A sputtered film; B SEM; B EPMA; C oxidation; C sulphidation; C selective oxidation

1. Introduction

Most alloys used as structural materials damage dramatically when exposed to atmospheres of low oxygen and relatively high sulfur partial pressures at high temperature, such as coal gasification [1]. Non protective sulphides grow fast on the surface of the alloy, resulting in the fast degeneration of the alloy [1]. For decades, researchers have devoted expenditure of time and effort on solving this problem. Binary alloys, such as Fe-Mn [2], Fe-Si [3], Fe-Y [4], Ni-Nb [5], Co-Y [6], Fe-Nb [7] are reported to fail to form the protective scale in atmospheres containing O and S. Therefore, the focus of the study transforms into the ternary alloys. The oxidation-sulphidation behaviors of ternary alloys are more complex than that of binary alloys [8]. Fe-Cr-Ni is reported to suffer a fast degeneration in H_2/H_2O/H_2S/Ar mixture [9]. Under specific circumstances, TiCrAl alloy could exhibit favorable corrosion resistance. For example, TiCrAl alloy possesses good corrosion resistance when Cr_2O_3 is thermodynamic stable [10]. The preparation of a protective coating on the surface of the alloy is a favorable way to improve the corrosion resistance of the substrate. Dudziak et al. [11] reported that multilayer CrAlYN/CrN coatings could induce a protective layer locally on Ti-45Al-8Nb in H_2/H_2S/H_2O mixture. Besides, Nano- or micro-coating is reported to be able to improve the oxidation/sulphidation resistance of the alloy [12].

According to our study about the oxidation of alloys, the formation of the protective oxide scale is important to the favorable corrosion resistance of the alloys exposed in harsh environment, and there are two ways to improve the formation of the

protective scale, such as SiO_2 and Cr_2O_3, on the surface of the alloy. First, we could raise the content of the Cr or Si in the alloy or prepare a coating containing high contents of Cr and Si on the surface of the alloy. For example, Bamba [13] and Guo [14] reported that the addition of Cr to Fe-Si alloy can induce the formation of SiO_2 layer in pure oxidizing atmosphere. Second, we also could decrease the grain size of the alloy to improve the outward diffusion of the Cr and Si to achieve the selective oxidation of Si and form the protective scale [11, 12]. In our previous study, the Fe-Si alloy exhibited poor corrosion resistance in the H_2-CO_2-H_2S at 700 ^oC [3], which is not acceptable. Therefore, we added 5 at. % Cr into the Fe-Si alloy and studied its corrosion behavior in this work. Furthermore, the micrograin coating with the same composition of the alloy was prepared on the surface of the as-cast alloy and its corrosion behavior at 700 ^oC was also studied.

2. Experimental procedure

A single phase α-Fe-Cr-Si alloy (Fe-5Cr-5Si, at.%) was prepared by vacuum induction melting technology. The purities of the raw materials are as following: 99.8% Fe, 99.99%Cr and 99.99% Si. Cast ingot was cut into samples with a size of 10×8×1.5 mm. A hole with a diameter of 1.5mm was drilled to suspend the sample. The samples were abraded successively down to 2000-grit SiC and cleaned. A coating with a thickness of about 17.5~20μm was deposited by magnetron sputtering technology with an SBH-511D DC system. The target with a size of 380×127×3 mm has the same composition as the as-cast alloy. The specimens were polished and ultrasonically cleaned in ethanol before sputtered. The parameters of the deposition process are shown in table 1.

The H_2-CO_2-H_2S mixture was used to simulate the coal gasification. The mixture is composed of (vol. %) 79.36 CO_2, 0.12 H_2S, balanced H_2 and was obtained by adding pure CO_2 and H_2 to H_2-1vol.% H_2S premixed gases in a cylinder by controlling their flowrates. The flowrates of gases are shown in table 2. The mixed gases passed through a chunk of Pt gauze before contacting the sample to help reach the thermodynamic equilibrium. According to the calculation with the help of the

software of Ivtanthermo, the equilibrium partial pressures of S_2 and O_2 at the experimental temperature are $l0^{-8}$ atm and 10^{-20} atm, respectively, which are identical to those in coal gasification.

Each corrosion test was carried out with a microbalance (Setaram B-92) for three times. The corrosion test procedure is as following: first, the sample is suspended in a quartz tube which is filled with the flowing reactive gases, and the furnace (Kittanning, PA 16207) is heated underneath; second, the vertical furnace is raised to the height of the quartz tube after reaching at the experiment temperature and the quartz tube is placed at the flat-temperature zone of the furnace. The temperature in the chamber of the furnace is controlled by a temperature controller (Thermcraft, P. O. Box 12037 3950 overdale Rd. Winston-salem, NC 27117, U.S.A.). The fluctuation of the test temperature is less than 5°C; finally, the sample cools down to the room temperature within the furnace after corrosion tests, and then is taken out for examination.

Corroded samples were examined by optical microscopy (OM, ZEISS observer A1M), X-ray diffraction (XRD, Panalytical X' Pert PRO, Cu Kα radiation at 40 kV, PA Analytical Almelo, Holland) and scanning electron microscopy (SEM, FEI INSPECT F 50, FEI, Hillsboro, OR) with energy dispersive X-ray analysis (EDX, OXFORD X-Max, Oxford Instruments Oxford, U.K.), as well as by electron probe micro-analysis (EPMA-1610, Shimadzu, Kyoto, Japan). In order to detect the phases in the whole inner layer of the scale, the corroded samples were alternately grinding off some corrosion compounds and then detected by XRD on the ground surface. Transmission electron microscope (TEM 2100F transmission electron microscope, JEOL) was used to study microstructure of the as-prepared sputtered film and X-ray photoelectron spectroscopy (XPS, ESCALAB250, Thermo, U.S.A.) was used to study the surfacial composition of the sputtered film.

3. Results

The microstructures of the Fe-5Cr-5Si alloy with and without the magnetron sputtered film are shown in Fig. 1. The as-cast alloy has typical equiaxed grains and

its average grain size is about 0.7 mm which is calculated according to GB/T 6394-2002 (Fig. 1a). The microstructure of the magnetron sputtered film is rather different from that of the as-cast alloy. The sputtered Fe-5Cr-5Si film shows a typical columnar grain structure with relatively loose grain boundaries, besides, micro-channels vertical to the surface are also noticeable, as shown in Fig. 1b and Fig. 1c. The thickness of the coating ranges from 17.5 to 20μm. The average grain size of the coating as measured by TEM is about 200 nm (Fig. 1d), which is much smaller than that of the as-cast alloy. The average compositions of the as-cast Fe-5Cr-5Si alloy and the sputtered film are shown in table 3. It can be seen that the actual compositions of the as-cast alloy and the sputtered film are close to the nominal composition (Fe-5Cr-5Si). The contents of Si, Cr and Fe at the actual surface of the sputtered film are also shown in table 3 and the enrichment of Si is observed.

The corrosion kinetics of the Fe-5Cr-5Si alloy with and without the coating corroded at 700^{o}C in the H_2-CO_2-H_2S up to 24 h are shown in Fig. 2, and their parabolic forms are shown in Fig. 3. The total mass gain of the as-cast alloy after 24 h corrosion at 700°C is about 33mg/cm^2 (Fig. 2). The corrosion kinetic of the as-cast alloy follows an approximately parabolic law at the initial stage, while the mass of the sample increases faster in the last stage and it seems that the kinetic law turns from the parabolic law to a linear law. Different from the as-cast alloy, the mass of the coated alloy increases fast in the first 3 h, but almost keeps as a constant in the latter stage. It is worth noting that the mass gain of the coated alloy in the first 3 h is even higher than that of the as-cast one. The total mass gain of the coated alloy after 24h corrosion at 700°C is about 10mg/cm^2, which is much less than that of the as-cast alloy. In addition, the parabolic form of the kinetic curve of the coated alloy after 3 h is a straight line, as shown in Fig.3, meaning that the kinetic of the coated alloy follows a simple parabolic law after 3 h, and the parabolic rate constant is extremely small, equal to 6.07×10^{-12} $g^2cm^{-4}s^{-1}$.

The XRD patterns of the as-cast Fe-5Cr-5Si alloy after 24 h corrosion in H_2-CO_2-H_2S at 700°C are shown in Fig. 4. The corroded samples were polished layer

by layer and detected by XRD on the ground surface to detect all the phases in the inner layer of the scale. The outer part of the scale is pure FeS, indicating the existing of a thick FeS layer. The phases in the inner part of the scale are much complex and composed of $FeCr_2O_4$, Fe_2SiO_4 and FeS. It should be noted that the content of the Fe_2SiO_4 in the innermost part of the scale is higher than that in the intermediate part of scale. Cross section (BEI) of the as-cast Fe-5Cr-5Si alloy after 24h corrosion in H_2-CO_2-H_2S mixture at 700^{o}C is shown in Fig. 5. The scale is composed of two layers, the outer layer is a columnar pure FeS layer, and a small trace of oxide of Cr is detected at the bottom of this layer. The inner layer is more complex and composed of FeS (light phase) and the spinels of Si and Cr (gray phases). The element mapping (Fe, Cr, Si, S, O) of the inner scale for the as-cast Fe-5Cr-5Si alloy after 24 h corrosion in H_2-CO_2-H_2S mixture at 700°C is shown in Fig. 6. Fe, Cr and Si almost evenly distribute in the inner layer of the scale, while the gradients of the contents of S and O with the depth of the scale are observed. The content of S in the inner layer decreases with the depth of the scale, on the contrary, the content of O increases with the depth of the scale.

The XRD patterns of the coated alloy after 24 h corrosion in H_2-CO_2-H_2S mixture at 700°C are shown in Fig. 7. The phases of the scale on the coated alloy are mainly composed of $FeCr_2O_4$, Fe_2SiO_4 and FeS, however, a small trace of Cr_2O_3 is detected in the innermost part of the scale. Cross section (BEI) of the coated Fe-5Cr-5Si alloy after 24 h corrosion in H_2-CO_2-H_2S mixture at 700^{o}C is shown in Fig. 8. The outer layer is FeS, and the inner layer is a mixed layer, composed of $FeCr_2O_4$, Fe_2SiO_4 and FeS. Beneath the mixed layer, a continuous layer with thickness of 1~2μm is observed. In order to better detect the composition of the thin layer, an electron probe micro-analysis (EPMA) test is conducted. The element mapping (Fe, Cr, Si, S, O) of the inner scale for the coated Fe-5Cr-5Si alloy after 24 h corrosion in H_2-CO_2-H_2S mixture at 700°C is shown in Fig. 9. With the increase of the depth of the scale, the content of S decreases and the content of O increases, which is similar to the element distribution of the inner scale of the as-cast alloy.

However, a thin layer rich in Cr, Si and O, but poor in Fe, is observed at the scale/alloy interface, indicating that the thin layer is mainly composed of Cr_2O_3 and SiO_2. Actually, the protective layer is at exactly the original coating/alloy interface, which could be verified by a shorter time corrosion. Cross section (BEI) of the coated Fe-5Cr-5Si alloys after 1 h corrosion in H_2-CO_2-H_2S mixture at 700^{o}C is shown in Fig. 10. A thick external FeS layer is observed, beneath which is a thin mixed layer composed of sulfides and oxides. Furthermore, there is an extremely thin layer rich in Cr, Si and O, which is probably Cr_2O_3 and SiO_2, is observed at the coating/alloy interface. Besides, an internal oxidation zone (ioz) of Si and Cr throughout the remaining sputtered film is observed.

In summary, the corrosion resistance of the as-cast Fe-5Cr-5Si alloy in H_2-CO_2-H_2S mixture at 700^{o}C is unacceptable, while its corrosion resistance can be improved evidently by deposited a sputtered film which has the same composition as the base alloy. The coating induces the formation of a continuous protective SiO_2+Cr_2O_3 layer at the original coating/alloy interface.

4. Discussion

4.1 Corrosion behavior of the as-cast Fe-5Cr-5Si alloy

A scale composed of FeS outer layer and FeS+$FeCr_2O_4$+Fe_2SiO_4 inner layer is formed on the as-cast Fe-5Cr-5Si alloy. All of FeS [3], SiO_2 [3] and Cr_2O_3 [8] are reported to be thermodynamically stable phases in contact with the H_2-CO_2-H_2S mixture. However, in this study, only FeS forms at the outer layer of the scale, indicating the growth rate of the FeS phase is much faster than that of the other phases. Young [15] reported that the growth rate of FeS is orders of magnitude larger than that of Cr_2O_3 and SiO_2. Therefore, the formation of oxides of Cr and Si in the outer layer is inhibited by the formation of FeS. Similar results have also been observed in the oxidation-sulphidation of Fe-Al alloys [16]. The growth of the outer layer of FeS is dominated by the outward diffusion of Fe, for the outward diffusion rate of Fe through FeS is orders of magnitude larger than the inward diffusion rate of S [17]. Beneath the FeS layer, mixtures of $FeCr_2O_4$, Fe_2SiO_4 and FeS are observed, indicating that oxygen

could diffuse through the FeS layer and react with the alloy. Considering that the lattice diffusion rate of oxygen in FeS is rather small, the diffusion of oxygen in FeS layer is probably through large numbers of vertical grain boundaries and defects in the FeS scale [18]. There are two sources of S for the growth of the FeS in the mixed layer, one diffuses from the gas phase through the outer layer of FeS, and the other is from the decomposition of FeS at the bottom of the FeS outer layer [3].

In our previous study, the corrosion behavior of Fe-5Si alloy in the same mixed gases was studied [3]. The corrosion scale of the Fe-5Si alloy is composed of an outer FeS layer, an inner FeS+SiO_2 mixed layer and an internal oxidation zone, which is similar to that of the as-cast Fe-5Cr-5Si alloy (Fig. 4), indicating the addition of 5 at. % Cr into the Fe-5Si alloy has little effect on the corrosion behavior of the alloy in H_2-CO_2-H_2S mixture.

4.2 Corrosion behavior of the coated Fe-5Cr-5Si alloy

For the coated alloy, the corrosion scale is more complex than that of the as-cast alloy. Beneath the outer layer of FeS and the intermediate layer of $FeCr_2O_4$＋Fe_2SiO_4 ＋FeS, a thin layer with thickness about 1~2μm composed of Cr_2O_3 and SiO_2 is observed at the original coating/alloy interface. Different from the fast growth of the mass gain of the as-cast alloy in the latter stage, the mass gain of the coated alloy barely changes after 3 h corrosion, indicating that the formation of the Cr_2O_3 and SiO_2 layer at the coating/alloy interface prevents the inward diffusion of the O and S [10] as well as the outward diffusion of Fe [19], and the further corrosion of the alloy is inhibited.

It is worth noting that the mass gain of the coated alloy increases fast at the initial stage of the corrosion test. There might be two reasons for the fast growth of the corrosion scale at the initial stage. First, because of the existence of the bulges and the hollows at the surface of the coating, the micrograin coating possesses much larger specific surface area than the as-cast alloy [20]. Second, a large density of grain boundaries and vertical clearances in the film supply short-circuit diffusion paths for the outward diffusion of Fe and inward diffusion of oxidants, resulting in the fast

corrosion of the sputtered film [21]. Moreover, it is proved that the scales growing on fine-grained materials generally tend to possess small grain sizes [22], which means there are sustained short-circuit diffusion paths for the inward diffusion of oxidants and outward diffusion of Fe. Therefore, the corrosion scale could grow fast at the initial stage until the coating is totally consumed.

It is reported that the magnetron sputtering technology may cause the enrichment of some elements at the actual surface of the film [23-25]. In the present study, the surfacial composition of the sputtered film is 32.8 at.% Si, 6.09 at.% Cr and 61.1 at.% Fe, much different from the average composition of the film. However, the enrichment of Si fails to promote the formation of the SiO_2 layer. Its effect on the corrosion behavior of the alloy needs further study.

4.3 Formation mechanism of the protective layer

For the coated alloy, it is interesting that a thin layer of SiO_2 and Cr_2O_3 forms at the coating/alloy interface. Similar result has never been reported before. Danielewski [26] reported that the inward diffusion rate of O through grain boundaries and vertical channels in the sputtered film is much faster than that of S, and the lattice diffusion rate of O in Fe is also faster than that of S. Therefore, it is reasonable to conclude that the inward diffusion rate of O in the sputtered film is faster than that of S. According to the research of J. Takada [27] and N. G. Ainslie [28], the diffusion rates (cm^2s^{-1}) of O and S in Fe are as following formulas:

$$D_O = 1.79 \times 10^{-3} \exp\left(\frac{-85700}{RT}\right) \quad (1)$$

$$D_S = 1.68 \exp\left(\frac{-204600}{RT}\right) \quad (2)$$

At 700°C, the diffusion coefficients of O and S in Fe are 1.059×10^{-7}, 1.74×10^{-11} cm^2s^{-1}, respectively. D_O is almost four orders of magtitude larger than D_S, which is corresponding to the fact that the diffusion front of O is deeper than that of S in the sputtered film. The diffusion rate of O in the sputtered coating is so fast that Cr and Si in the sputtered film is oxidized in situ, forming an internal oxidation zone (ioz) in the remaining coating, and the inward diffused S turns the ioz to the mixed corrosion

inner layer composed of oxides and sulphides subsequently.

When oxygen arrives at the original coating/alloy interface, selective oxidation of Si and Cr in the as-cast base alloy occurs due to the relatively low oxygen partial pressure, forming a protective layer of Cr_2O_3 and SiO_2 at the coating/alloy interface. The diffusion rate of S and O in the SiO_2 and Cr_2O_3 layer is so slow that the further inward diffusion of O and S is prevented; therefore, the further corrosion of the base alloy is inhibited.

Guo et al. [14] have studied the oxidation behavior of the as-cast Fe-5Cr-5Si alloy in H_2-CO_2 mixture with oxygen partial pressure equal to 10^{-20} atm at 700°C. Nodules composed of mixed oxides, rather than a protective SiO_2 and Cr_2O_3 scale, form at the surface of Fe-5Cr-5Si alloy, indicating that the contents of Cr and Si in Fe-5Cr-5Si alloy is not enough to form a protective oxide layer in the gas with oxygen partial pressure equal to 10^{-20} atm. Gesmundo et al. [29] has discussed the relationship between oxidation models of ternary A-B-C alloy (A<B<C, chemical activity) and the external oxygen pressure in pure oxidizing atmosphere, it is found that the lower the external oxygen pressure, the lower the critical contents of B and C needed to form their external scale. Combining the above two points, it can be deduced that the sputtered film decreases the partial pressure of oxygen at the coating/alloy interface from 10^{-20} atm to a certain degree and promotes the selective oxidation of Si and Cr in the base alloy.

The effects of the sputtered film could be divided into two parts, on one side, the sputtered film delays the inward diffusion of S and supplies a pure oxidizing atmosphere for the Fe-5Cr-5Si alloy, on the other side, the sputtered film decreases the oxygen partial pressure and promotes the selective oxidation of Cr and Si in the base alloy, forming a protective oxide layer at the coating/alloy interface. Thus, it is predicable that the sputtered film is able to provide good corrosion resistance for the Fe-5Cr-5Si alloy in H_2-CO_2-H_2S mixture.

5. Conclusion

The as-cast Fe-5Cr-5Si alloy suffers an unacceptable degeneration in H_2-CO_2-H_2S mixture at 700^oC. The scale is composed of an outer layer of FeS and an inner mixed layer of FeS+$FeCr_2O_4$+Fe_2SiO_4. The sputtered Fe-5Cr-5Si film improves the corrosion resistance of the as-cast Fe-5Cr-5Si alloy significantly. The film not only delays the inward diffusion of S, but also provides a pure oxidizing atmosphere for the base alloy with an oxygen partial pressure lower than that in the gas phase, leading to the selective oxidation of Si and Cr at the coating/alloy interface and forming a continuous protective layer of Cr_2O_3 and SiO_2, which is responsible for the sharp reduction of the corrosion rate of the coated alloy.

A financial supported by the NSFC (Projects N_O. 59071129 & 51501135) is gratefully acknowledged.

References

[1]. R. John, Sulfidation and Mixed Gas Corrosion of Alloys, in: T.J.A. Richardson (Ed.), Shreir's Corrosion, Elsevier, Oxford, 2010, pp. 240-271.

[2]. G. McAdam and D.J. Young, Mechanisms of the simultaneous sulfidation and oxidation of Fe-Mn alloys. Corros. Sci. 38 (1996) 247-266.

[3]. L.L. Liu, Q.Q. Guo, C.L. Zeng and Y. Niu, Corrosion of binary Fe-Si Alloys in reducing oxidizing and sulfidizing-oxidizing atmospheres at 700 ^oC，Oxd. Met. 81 (2014) 477-502.

[4]. Y. Niu, F. Gesmundo, R. Yan, and W. Wu, The corrosion of Fe-15 wt% Y and Fe-30 wt% Y in sulfidizing-oxidizing atmospheres at 600-800 ^oC. Corros. Sci. 41 (1999) 989-1012.

[5]. Y. Niu, F. Gesmundo, and F. Vinai, The oxidation-sulfidation of Ni-Nb alloys at 600-800 °C in H_2-H_2S-CO_2 mixtures. Corros. Sci. 37 (1995) 169-188.

[6]. Y. Niu, F. Gesmundo, and Y.S. Li, The corrosion of Co-15 wt.% Y at 600-800 degrees C in sulfidizing-oxidizing atmospheres. Oxd. Met. 51 (1999) 421-447.

[7]. Y. Niu, F. Gesmundo, and F. Viani, The oxidation-sulfidation of Fe-Nb alloys at 600-800^{o}C in H_2-H_2S-CO_2. Corros. Sci. 36 (1994) 1885-1906.

[8]. D. Young, Enabling theory, in: T. Burstein (eds.), High Temperature Oxidation and corrosion of Metals, Elsevier Corrosion Series, 2008, pp. 33

[9]. V. Srinivasan, R.A. Padgett Jr and A. Choudhury, Sulfidation behavior of Fe-25Cr-20Ni-Si in H_2 /H_2O/H_2S/Ar at 700^{o}C, Corros. 47 (1991) 703-711.

[10]. M.P. Brady, P.F. Tortorelli, K.L. More, and L.R. Walker, Sulfidation–oxidation behavior of FeCrAl and TiCrAl and the third-element effect. Oxd. Met. 74 (2010) 1-9.

[11]. T. Dudziak, H. L. Du, P. K. Datta, A. P. Ehiasarian and C. Reinhard, Enhanced sulphidation/oxidation resistance of Ti-45Al-8Nb alloy by nanostructured CrAlYN/CrN coatings at 750^{o}C, Mater. Corros. 65 (2014) 45-60.

[12]. P. F. Tortorelli, I. G. Wright, G. M. Goodwin, and M. Howell, High-Temperature Oxidation/Sulfidation Resistance of Iron-Aluminide Coatings, Elevated Temperature Coatings: Science and Technology II, Eds. N. B. Dahotre, and J. M. Hampikian, (Warrendale, PA: TMS, 1996), 175-185.

[13]. G. Bamba, Y. Wouters, A. Galerie, F. Charlot and A. Dellali, Thermal oxidation kinetics and oxide scale adhesion of Fe–15Cr alloys as a function of their silicon content, Acta Mater. 54 (2006) 3917-3922.

[14]. Q.Q. Guo, S. Liu, X.F. Wu, L.L. Liu and Y. Niu, Scaling behavior of two Fe-xCr-5Si alloys under high and low oxygen pressures at 700 °C, Corros. Sci. 10 (2015) 579-588.

[15]. D.J. Young and W.W. Smeltzer, Sulfidation Kinetics of Iron and Ferritic Iron- Cobalt Alloys. J. Electrochem. Soc. 123(1976) 229-234.

[16]. S.W. Banovic, J.N. DuPont and A.R. Marder, High temperature sulfidation behavior of low Al iron-aluminum compositions, Scripta Mater. 38 (1998) 1763-1767.

[17]. R. H. Condit, R. R. Hobbins and C. E. Birchenall, Self-Diffusion of Iron and Sulfur in Ferrous Sulfide, Oxid. Met. 8 (1974): 409 -455.

[18]. S. Mccormick, M.A. Dayananda and R.E. Grace, Diffusion-limited sulfidation of wustite, Metall. Mater. Trans. B, 6 (1975) 55-61.

[19]. A. Atkinson and J. W. Gardner, The diffusion of Fe^{3+} in amorphous SiO_2 and the protective properties of SiO_2 layers, Corros. Sci. 21 (1981) 49-58.

[20]. F. Wang, H. Lou, and W. Wu, The oxidation resistance of a sputtered, microcrystalline TiAl-intermetallic-compound film. Oxd. Met. 43(1995) 395-409.

[21] G. F. Chen and H. Y. Lou, Oxidation kinetics of sputtered Ni-5Cr-5Al nanocrystalline coating at 900 °C and 1000°C, NanoStruct. Mater. 11 (1999) 637–641.

[22]. R. K. Singh Raman, A.S. Khanna, R.K. Tiwari and J.B. Gnanamoorthy, Influence of grain size on the oxidation resistance of 2 4 1 Cr-1Mo steel, Oxd. Met. 37 (1992) 1-12.

[23]. M. Vorokhtaa, I. Khalakhana, M. Václavůa, G. Kovácsb, S. M. Kozlovb, P. Kúša, T. Skálaa, N. Tsuda, J.Lavkováa, V. Potinc, I. Matolínováa, K. M. Neymanb, V. Matolína, Surface composition of magnetron sputtered Pt-Co thin film catalyst for proton exchange membrane fuel cells, Appl. Surf. Sci. 365 (2016) 245-251.

[24]. S. K. Sharma and S. Mohan, Influence of annealing on structural, morphological, compositional and surface properties of magnetron sputtered nickel–titanium thin films, Appl. Surf. Sci. 282 (2013) 492–498

[25]. M.J. Chuang, H.F. Huang, C.H. Wen and A.K. Chu, On the structure and surface chemical composition of indium–tin oxide films prepared by long-throw magnetron sputtering, Thin Solid Films, 518 (2010) 2290–2294.

[26]. M. Danielewski, S. Mrowec and A. Stoklosa, Sulfidation of iron at high temperatures and diffusion kinetics in ferrous sulfide, Oxd. Met. 17 (1982) 77-97.

[27]. J. Takada and M. Adachi, Determination of diffusion-coefficient of oxygen in

alpha-iron from internal oxidation measurements in Fe-Si alloys, J. Mater. Sci. 21 (1986) 2133-2137.

[28]. N. G. Ainslie and A. U. Seybolt, Diffusion and solubility of sulphur in iron and silicon, Tetsu. To. Hagane. 194 (1960) 341-350.

[29]. F. Gesmundo and Y. Niu, The internal oxidation of ternary alloys. VII: The transition from the internal to the external oxidation of the two most-reactive components under intermediate oxidant pressures, Oxd. Met. 66 (2006) 69-89.

Figure captions

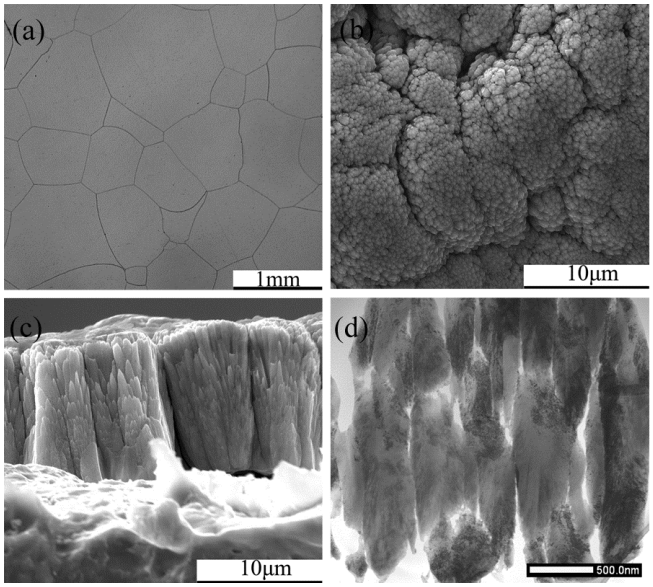

Fig. 1 Microstructure of the as-cast Fe-5Cr-5Si alloy with and without the sputtered Fe-5Cr-5Si film. (a) metallurgical structure (OM) of the as-cast Fe-5Cr-5Si alloy; (b) surface morphology (SEM) of the sputtered Fe-5Cr-5Si film; (c) cross section morphology (SEM) of the sputtered Fe-5Cr-5Si film; (d) bright field image (TEM) of the sputtered Fe-5Cr-5Si film.

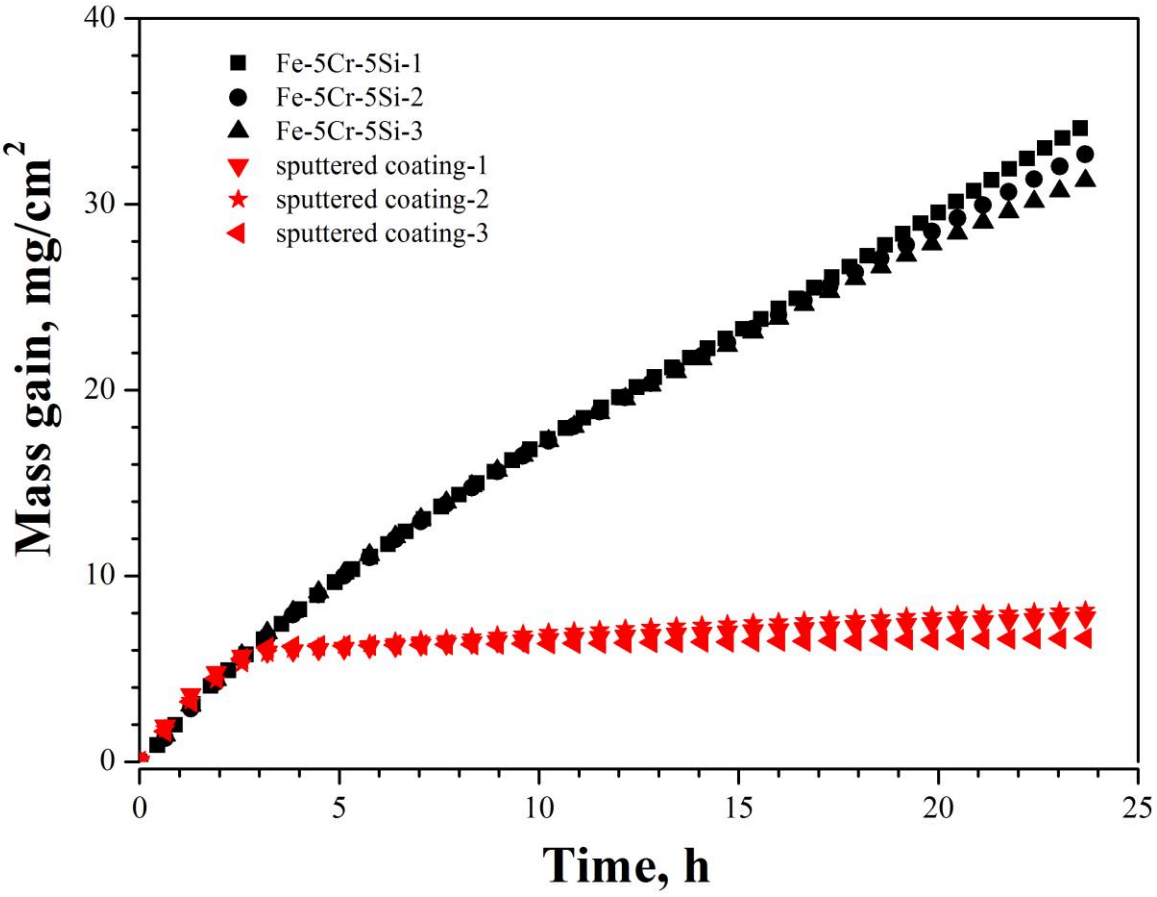

Fig. 2 Corrosion kinetic curves of the as-cast Fe-5Cr-5Si alloy with and without the sputtered Fe-5Cr-5Si film in H_2-CO_2-H_2S at 700 ºC for 24h. Each corrosion test was carried out for three times.

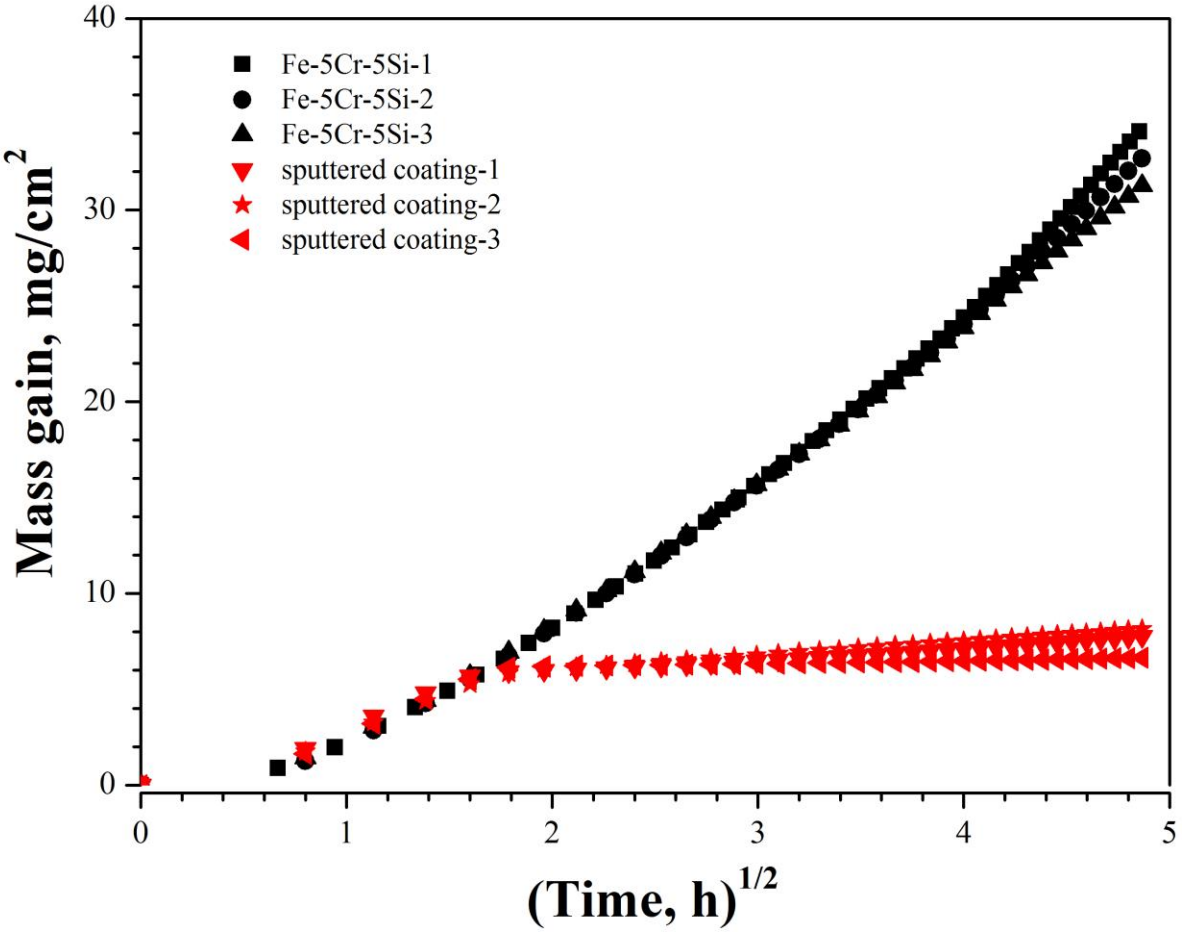

Fig. 3 Parabolic form of corrosion kinetic curves of the as-cast Fe-5Cr-5Si alloy with and without the sputtered Fe-5Cr-5Si film in H_2-CO_2-H_2S at 700 ^oC for 24h. Each corrosion test was carried out for three times.

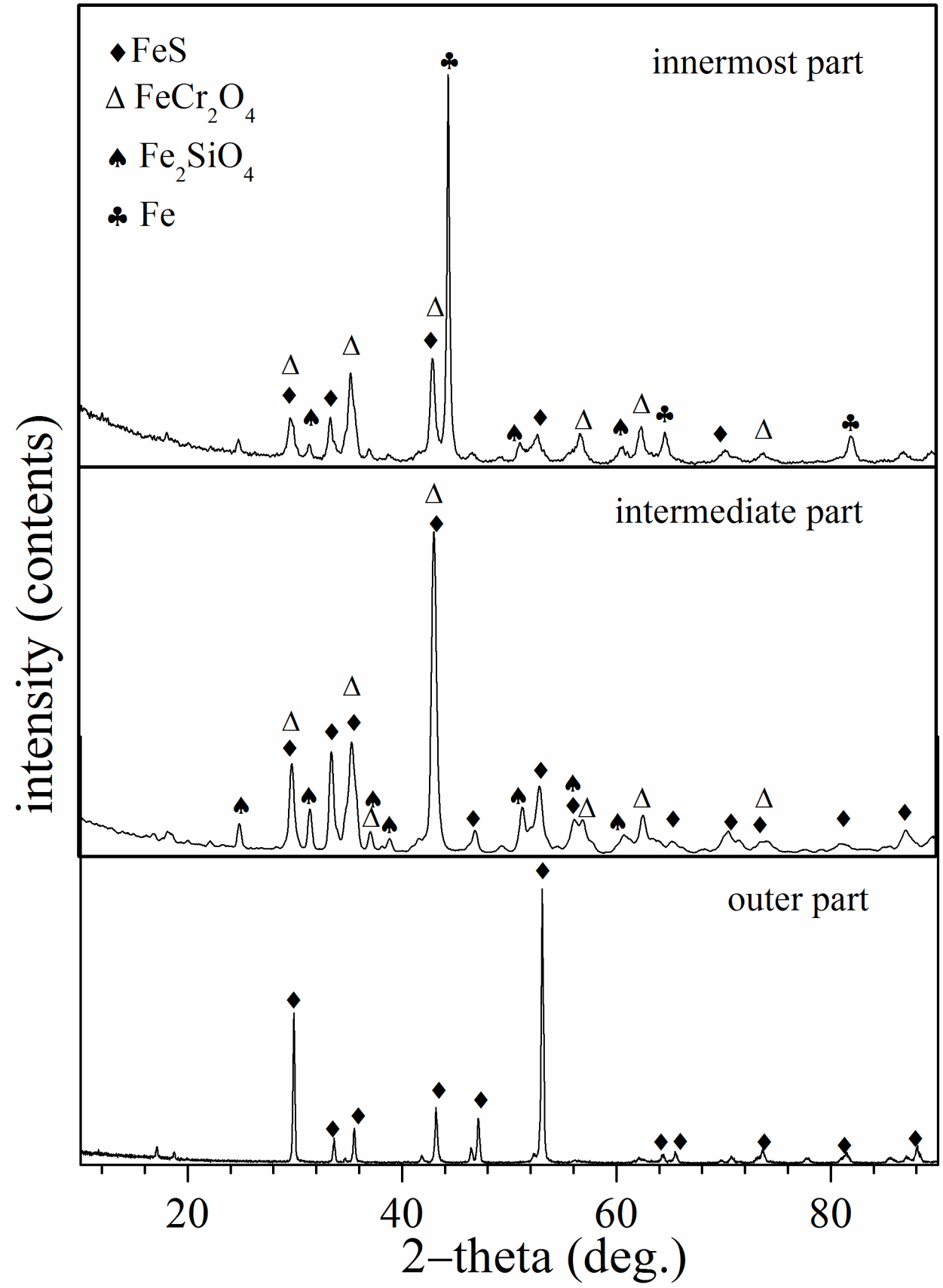

Fig. 4 XRD patterns for the as-cast Fe-5Cr-5Si alloy after 24h corrosion in H_2-CO_2-H_2S mixture at 700°C (polished for certain depths).

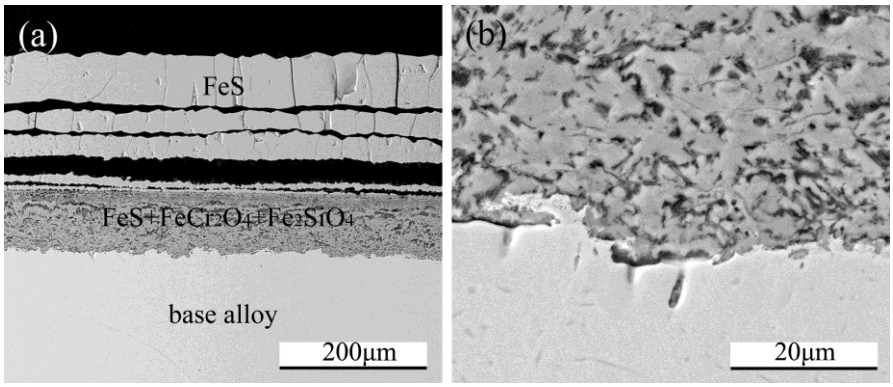

Fig. 5 Cross section (BEI) of the as-cast Fe-5Cr-5Si alloy after 24h corrosion in H_2-CO_2-H_2S mixture at 700^{o}C. (a) general view; (b) magnified view of inner scale.

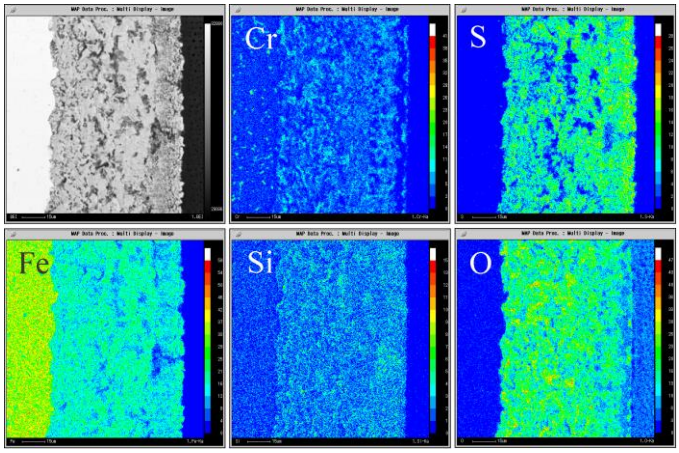

Fig. 6 Element mapping (Fe, Cr, Si, O, S) for the as-cast Fe-5Cr-5Si alloy after 24h corrosion in H_2-CO_2-H_2S mixture at 700^{o}C.

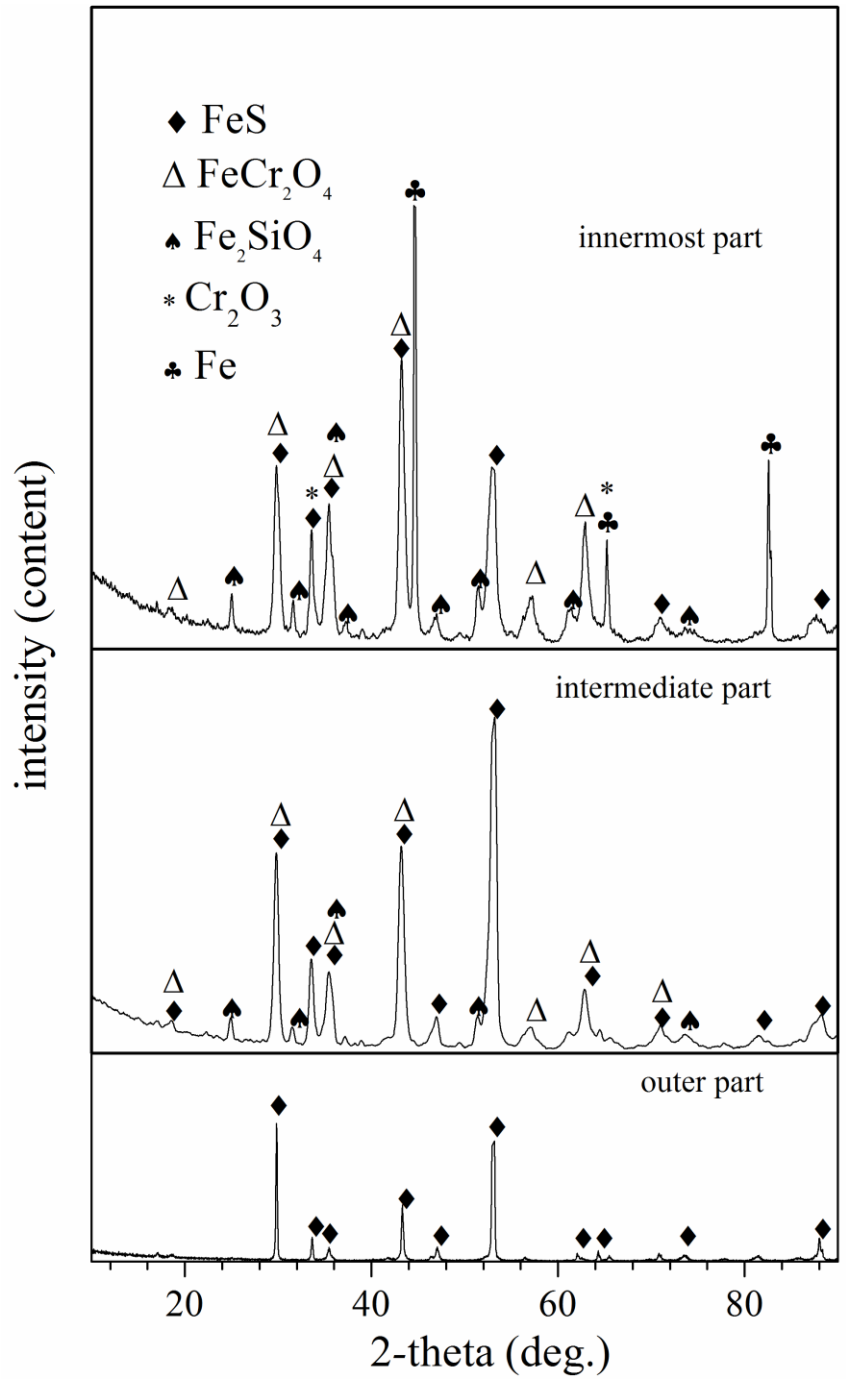

Fig. 7 XRD patterns for the coated Fe-5Cr-5Si alloy after 24h corrosion in H_2-CO_2-H_2S mixture at 700^oC (polished for certain depths).

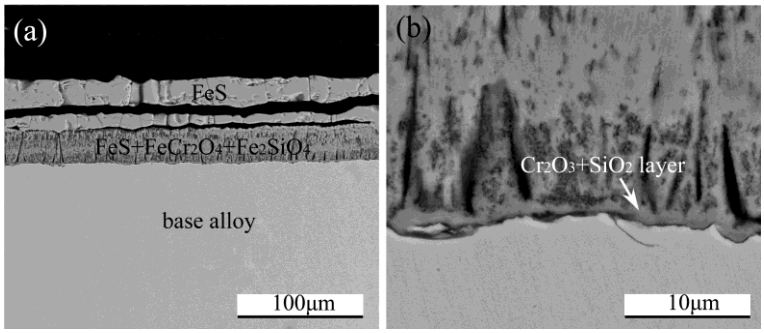

Fig. 8 Cross section (BEI) of the coated Fe-5Cr-5Si alloy after 24h corrosion in H_2-CO_2-H_2S mixture at 700°C. (a) general view; (b) magnified view of inner scale.

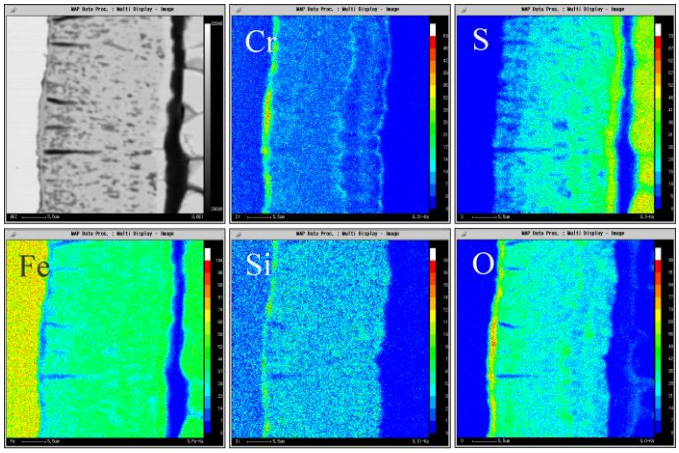

Fig. 9 Element mapping (Fe, Cr, Si, O, S) for the coated Fe-5Cr-5Si alloy after 24h corrosion in H_2-CO_2-H_2S mixture at 700^{o}C.

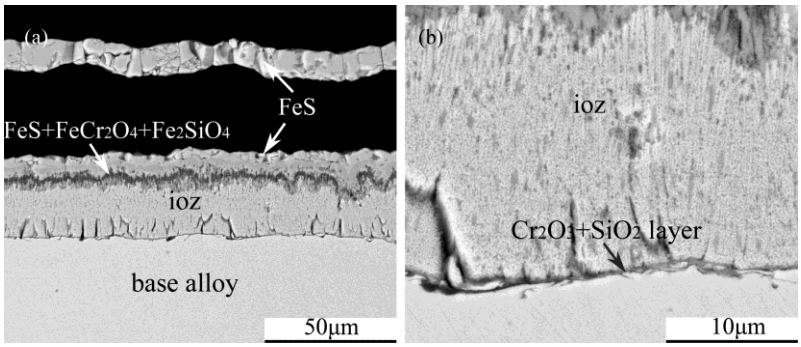

Fig. 10 Cross section (BEI) of the coated Fe-5Cr-5Si alloy after 1h corrosion in H_2-CO_2-H_2S mixture at 700°C. (a) general view; (b) magnified view of inner scale.

Table 1. The parameters of the deposition process

Parameter	Numerical value
sputtering duration	8 h
background vacuum	0.5×10^{-7} atm
argon pressure	0.25 Pa
substrate temperature	180 ^{o}C
sputtering voltage	700 ~750V
distance between sample and target	100mm

Table 2 the flowrates of the gases

Gases	CO_2	H_2	H_2-1vol.% H_2S	Total
Flowrates	79.36 ml/min	8.64 ml/min	12 ml/min	6L/h

Table 3. The average composition of the as-cast alloy and the sputtered film (detected by EDS), and the surfacial composition of the sputtered film (detected by XPS)

	Cr (at.%)	Si (at.%)	Fe (at.%)
average composition the as-cast alloy	4.19	4.77	91.04
average composition of the film	5.67	5.12	89.21
surfacial composition of the film	6.09	32.8	61.1